

Highly collimated broadside emission from room-temperature GaAs distributed Bragg reflector lasers^{a)}

W. Ng and A. Yariv

California Institute of Technology, Pasadena, California 91125
(Received 29 June 1977; accepted for publication 16 August 1977)

Highly collimated laser beams have been observed to be coupled out by second-order Bragg scattering from GaAs distributed Bragg reflector lasers. The beams are perpendicular to the waveguide plane and have an angular width of less than 1°. The diodes have a separate confinement structure and operate at room temperature with thresholds as low as 1.4 kA/cm².

PACS numbers: 42.82.+n, 42.55.Px, 42.80.Lt, 85.60.Jb

In this paper, we report the coupling of collimated broadside emission from room-temperature GaAs-GaAlAs lasers with low-loss Bragg reflectors. Recently reported¹ GaAs-GaAlAs distributed Bragg reflector (DBR) lasers were found to possess high threshold current densities due mostly to absorption losses in the unpumped grating section of the laser. In the work reported below, this problem has been reduced through the use of a separate confinement (SC) scheme in which a large part of the mode energy propagates in low-loss Ga_{0.88}Al_{0.12}As adjacent to the *p*-GaAs active layer. New threshold current densities as low as 1.4 kA/cm² at room temperature have been achieved. The grating section with a period of $\Lambda \sim 4936 \text{ \AA}$ plays a double role. It acts as a Bragg mirror in fourth order providing laser feedback and simultaneously, in second order, as an output coupler providing low-divergence (<1°) output beams at near-normal angles to the junction plane. DBR lasers that operate with gratings providing feedback in the third order were reported in Refs. 2-4. Grating coupled beams have also been observed previously from other heterojunction device structures.⁵⁻¹⁰

Figure 1(a) shows the asymmetric SC structure used in this series of experiments. The epilayers grown successively onto the *n* substrate by liquid-phase epitaxy were *n*-Ga_{0.7}Al_{0.3}As (~1-2 μm), *p*-GaAs (<0.3 μm), *p*-Ga_{0.88}Al_{0.12}As (0.3-0.7 μm), *p*-Ga_{0.7}Al_{0.3}As (1-2 μm), and *p*^{*}GaAs (~1 μm). Mesa etching was achieved in two steps: 4:1:1 (H₂SO₄:H₂O₂:H₂O) was used first to etch away the *p*^{*} contact layer. The exposed Ga_{0.7}Al_{0.3}As layer was then selectively etched down to the Ga_{0.88}Al_{0.12}As layer by a preferential etch (275 g KI:15 g I₂:750 cm³ H₂O). By the use of preferential etching, the trenching problem¹ at the edge of the mesa has been reduced to an insignificant amount, and better coupling between the guided wave and the gratings is obtained. It is interesting to note that a similar profile control problem in the fabrication of ridged stripes by ion-beam milling was reported recently.¹¹ We have found that by performing the etching at ~50 °C, an etched surface smooth enough for grating fabrication is obtained.

Shipley AZ1350B was then spun onto the wafers for lithographic exposure by either the 4579-Å line of the

argon laser or the 4416-Å line of the HeCd laser. The thickness of the photoresist, as checked by a Sloan Dektak, was ~1000 Å. The period of the gratings fabricated was ~4936 Å. Cr-Au was then evaporated in the form of a gold stripe for contact on the *p* side so that grating coupled light can be observed from the *p* side of the diode. Au-Ge was used for contacting the *n* side. Figure 1(b) shows the device structure after grating fabrication. The nonuniformity of the gratings near the edge of the mesa is due to the nonuniform photoresist coating there caused by the mesa step.

The use of the SC scheme, in which the inversion is limited to the *p*-GaAs region while a large part of the mode energy is in the *p*-Ga_{0.88}Al_{0.12}As, is especially important in the DBR laser in which a major component of the loss is due to absorption in the unpumped grating section. By the use of a thin GaAs recombination layer, the effective loss constant in the unpumped section is reduced by Γ , the fraction of the mode energy in the lossy *p*-GaAs layer. Thus the SC scheme increases the coupling constant (κ) and L_{eff} , the effective field pene-

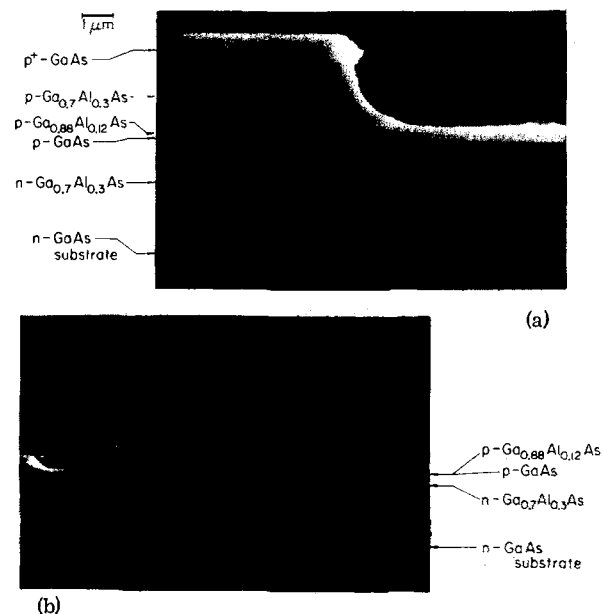


FIG. 1. (a) Cross section of mesa by SEM showing preferential etching down to *p*-Ga_{0.88}Al_{0.12}As. (b) Cross section of device structure after grating fabrication on both sides of mesa.

^{a)}Research supported by the Office of Naval Research and the National Science Foundation.

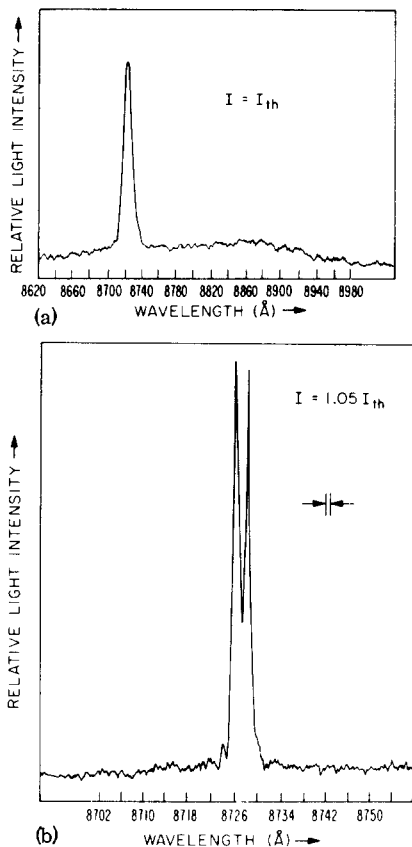


FIG. 2. (a) Low-resolution emission spectrum of one of the diodes showing lasing at the short-wavelength side of the spontaneous emission peak. (b) High-resolution emission spectrum of the same diode.

tration distance into the passive section because of the spread of the mode energy into the low-loss p -Ga_{0.88}Al_{0.12}As layer. The thin GaAs recombination layer also provides high gain or carrier inversion [$\sim (J/d)^m$, where $m = 1.5-3$]¹² in the central pumped section, where d is the active layer thickness.

The far-field divergence of the grating coupled light was observed by rotating a photomultiplier angularly around an axis centered on the diode. The photomultiplier was at a distance of ~ 30 cm from the diode and had a slit with a width ~ 0.7 mm, giving an angular resolution of $\sim 0.13^\circ$. The diodes were tested with driving pulses 100 nsec long at 140/sec. Typical threshold current densities were in the 2–4-kA/cm² range, but the lowest measured was 1.4 kA/cm².

The depth of the corrugation was typically 1500–1800 Å, and the estimated κ for distributed feedback was 20–50/cm. The effect of the corrugation on the emission spectrum is shown in Fig. 2(a). For this particular diode, lasing occurred with a threshold current density of 1.8 kA/cm² at the high-absorption side of the spontaneous emission peak. This is in contrast to the type of oscillation, reported¹³ for double-heterostructure diodes that had an unpumped but uncorrugated section, made possible by band-gap shrinkage under carrier injection. Figure 2(b) shows a high-resolution emission spectrum of the same diode at $I = 1.05I_{th}$. The mode spacing of ~ 2 Å agrees well with that calculated from

the experimentally determined cavity length of ~ 425 μ . The oscillation was typically limited to two or three modes near threshold, showing the frequency selectivity provided by the Bragg reflectors. When the quality of the grating was spoiled by scribing the diode surface with a rough edge, the diode did not lase up to an injection current density of 10 kA/cm², showing that corrugations giving a high κ were necessary to provide feedback for low-threshold operation. The differential quantum efficiency of these diodes was between 10^{-2} and 10^{-3} , with a typical value of 4×10^{-3} , taking into account the power of the grating coupled beam as well as that from one end of the diode.

Figure 3(a) shows the far-field distribution of D4. The full width at half-maximum of the coupled beam is less than 1° . The beam was collimated at lower pumping currents but had a smaller magnitude. From the fact that a single peak was observed at 90° to the junction plane it follows that the period Λ and the laser wavelength λ are related by

$$\Lambda = 2(\lambda/n_{eff}),$$

where n_{eff} is the effective mode index of refraction (i. e., $\lambda/n_{eff} =$ guide wavelength). The above relation is also the condition for Bragg retroreflection in fourth order ($m = 4$) so that the grating doubles as a reflector and a coupler. The effective mode index at $\lambda = 8710$ Å is 3.53. The power coupled out by a radiation aperture with an area of $1.2 \times 10^5 \mu^2$ was ~ 3.5 mW, and was typical of these diodes.

The emission spectrum taken from one end of the diode at threshold is shown in Fig. 3(b). The lasing bandwidth was 2 Å or less, and the threshold current density was 1.4 kA/cm². At 3.5 times the threshold current, the spectral width centered at ~ 8710 Å broad-

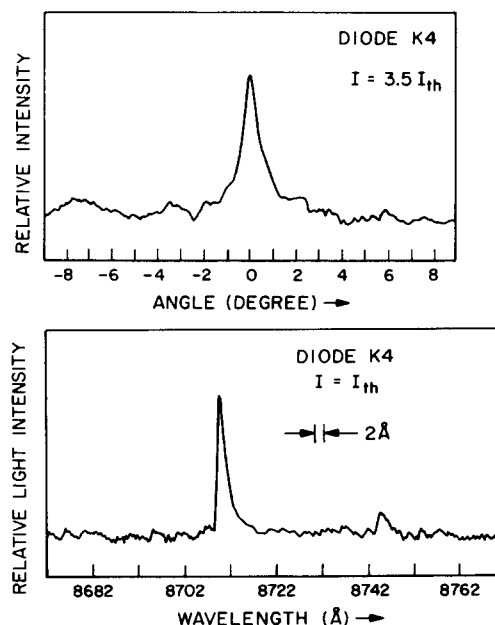


FIG. 3. (a) Far-field distribution of grating coupled light of K4 at near-normal angles ($I = 3.5I_{th}$). (b) Emission spectrum of K4 at threshold from one end of the diode.

ened to $\sim 8 \text{ \AA}$ at the high-absorption side of the spontaneous emission peak. The gratings had lengths of 200 and 600μ , and the light coupled out was observed from the longer section. One end, corresponding to that of the longer passive section, was cleaved. The other end was saw cut to destroy the reflectivity. The spectral width of $\sim 8 \text{ \AA}$ accounts for $\sim 0.25^\circ$ of the observed angular width. The exponential-like decay of the laser field in the corrugated section constitutes another (angular) broadening mechanism which may account for the difference.

In conclusion, we have demonstrated distributed feedback and output coupling at normal angles to the junction plane from DBR lasers using fourth-order gratings. Device fabrication and operation is improved by the use of preferential etching and the adoption of a separate confinement structure. The latter makes for better coupling between the guided wave and the gratings, and reduces the loss in the unpumped section of the diode. The grating coupled beams are highly collimated as expected and low room-temperature

thresholds down to 1.4 kA/cm^2 have been observed.

- ¹W. Ng, H.W. Yen, A. Katzir, I. Samid, and A. Yariv, *Appl. Phys. Lett.* **29**, 684 (1976).
- ²F.K. Reinhart, R.A. Logan, and C.V. Shank, *Appl. Phys. Lett.* **27**, 45 (1975).
- ³W. T. Tsang and S. Wang, *Appl. Phys. Lett.* **28**, 596 (1976).
- ⁴Hirofumi Namizaki, Mohammad Kazem Shams, and Shyh Wang, *Appl. Phys. Lett.* **31**, 121 (1977).
- ⁵D.R. Scifres, R.D. Burnham, and W. Streifer, *Appl. Phys. Lett.* **26**, 48 (1975).
- ⁶Zh. I. Alferov, V.M. Andreyev, S.A. Gurevich, R.F. Kazarinov, V.R. Farionov, M.N. Mizerov, and E.L. Portnoy, *IEEE J. Quantum Electron.* **QE-11**, 449 (1975).
- ⁷P. Zory and L.D. Comerford, *IEEE J. Quantum Electron.* **QE-11**, 451 (1975).
- ⁸R.D. Burnham, D.R. Scifres, and W. Streifer, *Appl. Phys. Lett.* **26**, 644 (1975).
- ⁹D.R. Scifres, R.D. Burnham, and W. Streifer, *Appl. Phys. Lett.* **27**, 295 (1975).
- ¹⁰D.R. Scifres, R.D. Burnham, and W. Streifer, *Appl. Phys. Lett.* **28**, 681 (1976).
- ¹¹S. Somekh and H.C. Casey, Jr., *Appl. Opt.* **16**, 126 (1977).
- ¹²M. B. Panish, *Proc. IEEE* **64**, 1512 (1976).
- ¹³Kunia Kira Iwamoto and Isao Hino, *J. Appl. Phys.* **48**, 1742 (1977).

Thin-film machining by laser-induced explosion

Vincent J. Zaleckas

Western Electric Company, Engineering Research Center, P.O. Box 900, Princeton, New Jersey 08540

Jackson C. Koo^{a)}

Instituto de Fisica, Unicamp C.P. 1170, Campinas 13.100 S.P., Brasil
(Received 11 April 1977; accepted for publication 19 August 1977)

This paper describes a process for the laser machining of thin metallic films on dielectric substrates. The observation of a distinct minimum in the machining threshold and the fact that no substrate damage occurs over a wide range of incident power are explained based on an explosive film-removal mechanism. Experimental results supporting the predictions are presented.

PACS numbers: 79.20.Ds, 78.65.-s, 42.60.-v, 44.10.+r

In the past, the basic mechanism considered in machining applications of thin films has been the direct evaporation of the metallic film through optical radiation heating.¹ Under such conditions, the minimum optical energy required for the removal of a particular metallic film, i. e., the threshold value for laser machining, is dependent not only upon the optical properties but also the thermal properties such as the evaporation temperature and the latent heat of evaporation of the metallic film. For many applications, films such as copper, zinc, or gold are typically used. Because of the relatively high evaporation temperatures of these films, a direct evaporation mechanism would predict laser machining thresholds which could damage heat-sensitive substrates.

For the machining of copper on epoxy, an alternative film removal mechanism is presented which accounts for the observed experimental results discussed in the report; namely,

(a) for film thicknesses less than a few thousand angstroms, machining thresholds significantly less than that predicted by a direct evaporation process are observed;

(b) a distinct minimum exists in the laser machining threshold as a function of film thickness;

(c) no substrate damage, defined either as a physical damage such as craterlike formations or alterations to physical properties such as resistivity, is observed over a wide range of laser power.

As in the case of direct evaporation, the temperature of the metallic film and that of the underlying dielectric substrate will rise due to absorption of the incident

^{a)}Formerly with Western Electric Co., Princeton, N.J.